Determination of sizes of spherical particles, prepared by dispersion polymerization of methyl methacrylate in non-aqueous medium, by analysis of the particle scattering and autocorrelation functions

Martin Helmstedt* and Hartmut Schäfer
Fachbereich Physik, Universität Leipzig, Linnestrasse 5, D-04103 Leipzig, Germany

Particle masses of the order of 10^8–10^{10} g mol^{-1} and the radii of gyration and hydrodynamic radii of spherical poly(methyl methacrylate) particles were characterized by combined static and dynamic light scattering. The dispersions were prepared by dispersion polymerization and stabilized by polystyrene-*block*-poly(ethylene-*co*-propylene). The radii of gyration were calculated from the measured particle scattering intensity by fitting procedures using the Rayleigh formula for spheres. This practice allows the use of all points actually measured instead of the uncertain values at low angles only. The strongly disturbing influence of small contents of large particles (aggregated particles, dust) was eliminated. The autocorrelation functions were measured by dynamic light scattering and analysed by the Contin procedure. The coronas and densities of the particles could be characterized on the basis of the geometric radii of the pure main components.

(Keywords: light scattering; poly(methyl methacrylate); block copolymers)

INTRODUCTION

Dispersion polymerization is a modified precipitation polymerization technique[1] carried out in the presence of stabilizer which prevents the macroscopic separation of the polymer. The monomer to be polymerized must be soluble in the dispersion medium and the forming polymer must be insoluble. Block or graft copolymers are normally used as steric stabilizers[1,2]. The best stabilizing effect can be obtained if the blocks of one type are insoluble in the reaction medium (the so-called anchor blocks, *Figure 1*) and if the blocks of the other type are soluble and form the shell ('corona') of the dispersion particle.

In the submicrometre range in particular, the light scattering technique is a powerful tool for the investigation of dispersion particles. By means of static light scattering, absolute values of molar masses of the particles and their radius of gyration can be obtained. The hydrodynamic radius, defined as the radius of the sphere with equal hydrodynamic behaviour, can be determined by dynamic light scattering.

In a previous study[3] we obtained the molar masses, radii of gyration, and the volume fraction of the solvent in the particle body of selected poly(methyl methacrylate) (PMMA) dispersions stabilized by polystyrene-*block*-poly(ethylene-*co*-propylene) in decane. In this contribution we analyse the possibility of fitting the particle scattering function of homogeneous spheres to experimental data. By combining with a mathematical separation procedure and with results of dynamic light scattering, it is possible to determine the corona density on the assumption of an unswollen particle core.

Determination of particle masses and radii of gyration by two-component separation or a maximum fit

Two-component separation procedures are well established for the separation of molecular and 'microgel' components of solutions of macromolecules[4–9]. All these procedures are based on observation of the rapid decrease of the scattering intensity of a small amount of relatively

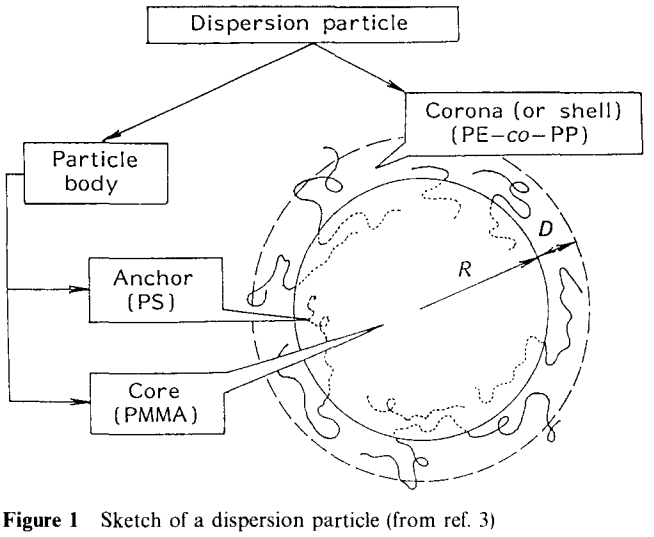

Figure 1 Sketch of a dispersion particle (from ref. 3)

* To whom correspondence should be addressed

0032-3861/94/16/3377-07

large particles in the wide-angle region, where the scattering of the main component with a smaller size dominates.

The basic assumptions for the two-component separation are:

$$w_1 + w_2 = 1 \tag{1}$$

and

$$M_1^* + M_2^* = M_w = (K_C/R_\Theta)^{-1} \tag{2}$$

where $w_{1,2}$ are the weight fractions of the main component 1, the 'normal' dispersion particles, and of the component 2. The nature of this component will be discussed later. Both components are assumed to be monodisperse. The asterisks represent apparent particle masses:

$$w_{1,2} M_{1,2} = M_{1,2}^* \tag{3}$$

It is useful to fit the data K_C/R_Θ (measured at various angles and extrapolated to infinite dilution), similarly to the method of Francuskiewicz and Dautzenberg[8]. But whereas these authors approximated the main component (macromolecules) by a $P(\Theta)$ function of polymer coils, we use Rayleigh's formula for the scattering of spheres[10] in order to approximate the main component, the spherical particles of the dispersions:

$$P(\Theta) = [(3/X^3)(\sin X - X \cos X)]^2 \tag{4}$$

with

$$X = (5/3)^{1/2}(4\pi n_0/\lambda_0) R_G \sin(\Theta/2) \tag{5}$$

In this simplified treatment we suppose that the particles are uniform and R_G is their radius of gyration. Knowledge of the R_G/M_w relation is required.

The model calculations can be started using the radii of gyration and the particle masses, which are estimated from the hydrodynamic radii and the experimental values M_w. By computer simulation combinations of R_G and M_w were rapidly found that fitted well with the experimental points of the angular dependence of K_C/R in the wide-angle range by equation (4). If the aim of the separation is a good fit for the main component 1, the criterion is a minimum of the difference between the measured and the calculated values at the same angle.

The advantages of this practice are:

1. A fit with the Rayleigh approximation gives better results than the use of simple polynomial functions.
2. The unmeasurable part in the low-angle region is completed by more exact values, which is especially significant for increasingly large particles.
3. At small angles of observation the presence of dust or aggregates strongly influences the scattering intensity. In the wide-angle region one obtains more exact values for particle masses and the radii of gyration, because the intensity of disturbing particles decreases to less than 1% in the wide-angle region. This limit is smaller than the experimental error, which we can assume to be about 2–3% for these strongly scattering particles.

For particles with a geometric radius greater than 140 nm, maxima and minima of K_C/R_Θ are observed in the 'window of observation' between 30 and 150°. In this region the calculation can be done with the Rayleigh–Debye–Gans approximation. (The Mie region begins at about 300 nm.) The fit of the position of the maxima is a second possibility for interpreting the experimental results. Details of both procedures are given in the Results and Discussion section.

EXPERIMENTAL

For dispersion polymerization and scanning electron microscopy, see references 3 and 11. The mass fraction of the stabilizer x_S of all samples is presented in *Table 1*. The ratio between the mass fractions of anchor and shell chains, $x_A:x_C = 0.418$, is constant for all samples.

Refractive index increments

By analogy with references 3 and 11, the refractive index increments of PMMA dispersions in decane at wavelength $\lambda_0 = 546$ (or 633) nm at 25°C were calculated according to the simple additivity rule:

$$v = v_S x_S + v_P(1 - x_S) \tag{6}$$

where x_S is the mass fraction of the steric stabilizer in the dispersed particles, v_S (= 0.120 (0.117) cm^3 g^{-1}) is the refractive index increment of the stabilizer determined by means of a Brice-Phoenix differential refractometer (BP-2000-V). The refractive index increment of the PMMA, $v_P = 0.081$ (0.078) cm^3 g^{-1}, was estimated by interpolation of literature data[12], that of polystyrene anchor blocks to $v_A = 0.169$ (0.165) cm^3 g^{-1} and that of shell chains to $v_C = 0.085$ (0.082) cm^3 g^{-1}.

Static light scattering (SLS)

The dispersions were diluted from 1:400 ('X' samples) to 1:10 000 (samples 13, 14 and 15) using purified decane (distillation and filtration over 1 μm glass filter) and filtered through filters of pore size 0.85 μm (Synpor 4, Labora, Czech Republic). The intensity of the scattered light was measured by means of a Fica 50 apparatus using a mercury high pressure lamp and wavelength $\lambda_0 = 546$ nm. Normally this apparatus allows the determination of intensity at 11–13 standard angles between 30 and 150°. Measurements at other angles can also be made. A neutral attenuator was used to decrease the high intensity of the scattered light. The Fica apparatus was calibrated using a sealed sample of

Table 1 Mass fractions of stabilizer x_S, particle masses M_w, radii of gyration R_G, and hydrodynamic radii R_H of poly(methyl methacrylate) dispersions in n-decane

Sample	x_S	$10^{-8} M_w$ (g mol^{-1})	R_G (nm)	R_H (nm)
X1	0.110	1.95	51.5	71.8
X2	0.199	0.71	47.1	61.6
X3	0.271	0.53	44.8	57.3
X4	0.332	0.38	44.7	53.8
1	0.054	9.30	157	89.1
2	0.102	2.35	66.4	69.0
3	0.146	1.10	48.2	65.0
4	0.185	0.91	46.5	67.6
5	0.035	43.8	200	151
6	0.068	13.4	71.3	121
7	0.098	6.4	59.2	98.5
8	0.127	4.0	39.0	91.5
9	0.026	84	199	174
10	0.052	50	146	175
11	0.076	65	128	180
12	0.098	37	86.2	161
13	0.022	246	295	191
14	0.042	257	349	198
15	0.062	206	325	180

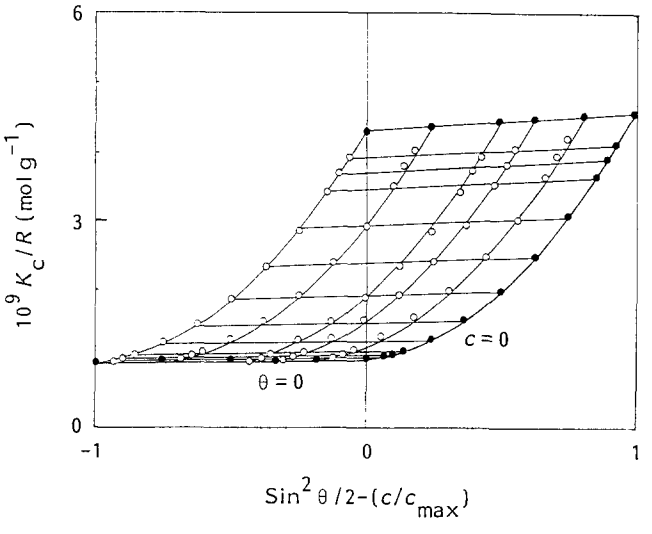

Figure 2 Zimm plot for dispersion of sample 6

high-purity benzene. Some samples were measured with a modified Sofica 42000 apparatus using a Zeiss 50 mW He–Ne laser ($\lambda_0 = 633$ nm) as the light source. Comparable results were obtained from the two types of apparatus.

The concentration dependence was very low in most cases, that is, $A_2 < 10^{-5}$ mol cm^3 g^{-1} (see *Figure 2*); this value could consequently be neglected.

Dynamic light scattering (DLS)

A laboratory-made homodyne light scattering spectrometer was used. It consisted mainly of the Sofica apparatus described above, the 50 mW He–Ne laser and an NSA 1000 100-channel stochastic analyser NSA 1000 (Metrimpex, Hungary) interfaced with a microcomputer and other peripheral units[13]. The autocorrelation functions were analysed by a single-exponential fit and by a non-negative least-squares procedure[14].

Some selected samples were independently measured by means of the laboratory-made homodyne spectrometer with a 96-channel digital correlator[3] and analysed by a single-exponential fit and by the Contin procedure. In all cases the hydrodynamic radii R_H were calculated from the diffusion coefficients, D_C, of the dispersion particles using the Stokes–Einstein equation:

$$R_H = kT/6\pi\eta D_C \qquad (7)$$

where k is the Boltzmann constant and η is the viscosity of decane at 25°C (=0.853 cP)[15]. The concentration dependence of the diffusion coefficient was neglected.

RESULTS AND DISCUSSION

Stability of diluted samples

According to the different stabilizer contents of the samples, the long-time stability of diluted dispersions is very different. The lowest concentration, which is practically stable for several hours to facilitate the measurement, varies with the stabilizer content of the dispersion particles and should be determined experimentally. We often used the concentration of 2×10^{-5} g ml^{-1} as the lower limit. An impressive example of the intensity changes with time is given in *Figure 3*. This effect is observed mainly for relatively unstable dispersions, that is the dispersions of samples 5, 9, 13, 14 and 15 with a high mass and — relative to the mass — low stabilizer content.

The scattering intensity of the diluted dispersion of higher concentration (a in *Figure 3*) is stable for 7 days or more, whereas the intensity of more (than the given concentration limit) dilute dispersions (b in *Figure 3*) decreases immediately. For example, in comparison with dissolved macromolecules, the scattering intensity of the compact dispersion particles is high. The possibility of multiple scattering[16] increases with increasing concentration. This fixed the upper concentration limit in the order of 3×10^{-4}–5×10^{-4} g ml^{-1}.

Finally, it is necessary to consider the aggregation and the change of the values K_C/R_Θ, which were plotted for the interpretation of SLS experiments. The precipitation of aggregated particles reduces the real concentration. In most cases, the particle masses obtained some hours or days after the dilution and filtration were apparently lowered. The particle dimensions, on the other hand, will be found higher than expected because aggregates influence the low-angle region, which is used for determining the radii of gyration.

To obey the rules for dilution, given above, and to measure these unstable samples immediately (i.e. for some minutes) after dilution is the best way to obtain correct results, especially for the dispersions with high mass and low stabilizer content.

Particle masses and hydrodynamic radii

The basic results from the static and dynamic measurements are arranged in *Table 1* together with the chemical composition parameters of all samples. The molar masses were obtained by a polynomial extrapolation of K_C/R_C to zero angle; the radii of gyration were obtained in the usual manner from the slope of this extrapolation curve. These data result from measurements that are independent of those given in references 3 and 11. In general they agree well. Both radii are plotted *versus* M_w in *Figure 4*. The linear regression analysis for log R_G and log R_H, respectively, *versus* log M_w gives the relations:

$$R_G = 0.132 M_w^{0.317}\ (\text{nm})$$

$$R_H = 1.212 M_w^{0.218}\ (\text{nm})$$

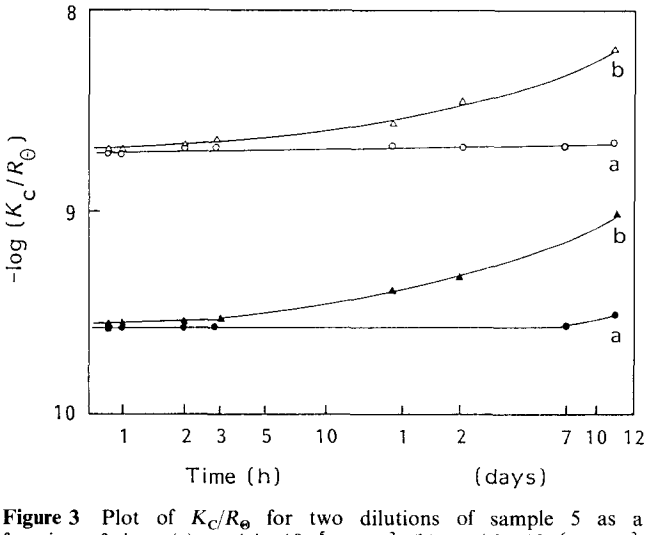

Figure 3 Plot of K_C/R_Θ for two dilutions of sample 5 as a function of time: (a) $c = 4.4 \times 10^{-5}$ g cm^{-3}; (b) $c = 4.3 \times 10^{-6}$ g cm^{-3}. ○, Δ, Measured at 90°; ●, ▲, measured at 11 preset angles (30–150°) and extrapolated to 0°

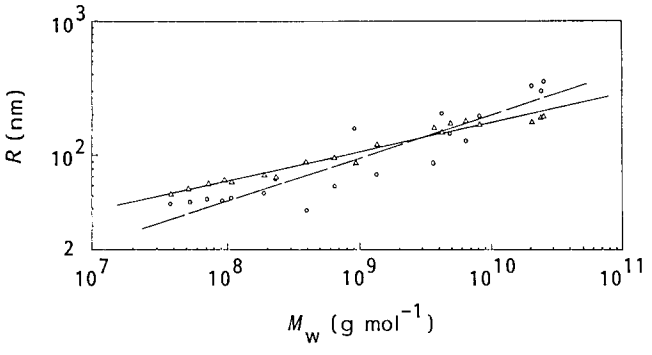

Figure 4 The radius of gyration R_G (○) and the hydrodynamic radius R_H (△) *versus* the particle mass M_w

with relatively low coefficients of correlation, $k_C^2 = 0.841$ or 0.942, respectively, especially in the case of R_G. The values represent particles with different stabilizer content and tendency to aggregate, which mainly influences the intensity of the scattered light.

According to the stabilizer content, the dispersion particles are neither 'hard' nor homogeneous spheres. Therefore not only the hydrodynamic but also the geometric radius is significant for obtaining further information on the density of the particles, their bodies and shells. The good correlation of R_H data and the poor correlation of R_G suggests a critical observation or, better, a correction of the SLS results by means of a two-component separation fit.

Two-component separation

By computer simulation, using the radii of gyration and particle masses estimated from the hydrodynamic radii and the experimental values of M_w, combinations of R_G and M_w were rapidly found that fitted well with the experimental data K_C/R_Θ by equation (4). A first approximation is the relation between R_G and M_w. In all cases, good agreement between 60° and 150° was obtained. This means a minimal difference of about 1% between the measured K_C/R_Θ and the calculated values. For light scattering intensity measurements it is normally smaller than the reproducibility range. The observed values of the samples with a low stabilizer content differed more strongly from the calculated values, and at smaller angles of observation the agreement varied.

In most cases we were not able to approximate all points by one component because in the small-angle range the residue is more than 1% of the intensity. The justification for the two-component separation fit is demonstrated by *Figure 5*, exemplified by sample 1. The difference between the simple polynomial extrapolation of the SLS data and the two-component fit is outside the experimental error. In the discussion we have to distinguish between samples X1–8 and 12 on the one side and samples 9–11 and 13–15 on the other.

Let us consider the first group of samples. The data obtained for this group are $R_{G,1}$ and M_1^*. $M_{w,1}$ was calculated by equation (3) and is listed instead of M_1^* in *Table 2*.

The equation

$$R_{G,1} = 7.30 \times 10^{-2} M_{w,1}^{0.328} \text{ (nm)}$$

with $k_C^2 = 0.990$, was obtained by a linear regression of the logarithmic data. The value for the exponent is slightly lower than that expected for hard spheres, owing to the dissolved corona of the particles. The relationship is valid up to $M \approx 2 \times 10^8$ g mol^{-1} and gives an average over all particles with various shells and for a broad spectrum of particle sizes (see *Figure 8*). For groups of samples with approximately the same mass fraction of stabilizer x_S, one can calculate similar relationships. For $x_S = 0.035$–0.068 the exponent is 0.340, for $x_S = 0.098$–0.145 it is 0.278 and for $x_S = 0.185$–0.331 it is 0.270. The exponents show the different interaction of the particles with the solvent according to the various content of stabilizing macromolecules.

Nevertheless, it is necessary to investigate whether one can interpret the main parts with real particle size distributions, which deviate more or less from the monodispersity. Therefore let us compare our results with published electron microscopic data of selected samples[3]. All of our $R_{G,1}$ values (converted into the geometric radii by multiplication by the factor $(5/3)^{1/2} = 1.291$) approximately represent the most frequently occurring large particles in the dispersions. This is understandable if we bear in mind that all radii determined by light scattering are z-averaged. In all cases, the difference points form a 'curve' of the angular dependence of intensity, similar to that of a spherical scatterer with distinctly larger particles. Obviously these points can also be described by equations (4) and (5). Therefore we also fitted these difference or 'residue' points by Rayleigh's formula necessary for spheres with radii that are two or three times larger than those of component 1. These values do not describe a second component of a real distribution, but describe aggregates, single particles of untypical size or some residual dust particles. Therefore it is more important to obtain corrected data for the first (or main) component than to characterize the small (and here unimportant) second component.

The weight fractions of this component are $0.0002 < w_2 < 0.0067$. For samples 1 and 5, with a small stabilizer content, the weight fraction of the aggregates is in the order of $w_2 \approx 0.03$, i.e. 3%. This is in agreement with the lower stability of the dispersions diluted for measurements. Only if equations (2) and (3) are nearly fulfilled and both curves are fitted by equations (4) and (5), is a coherent picture, including all samples X1–8 and 12, obtained.

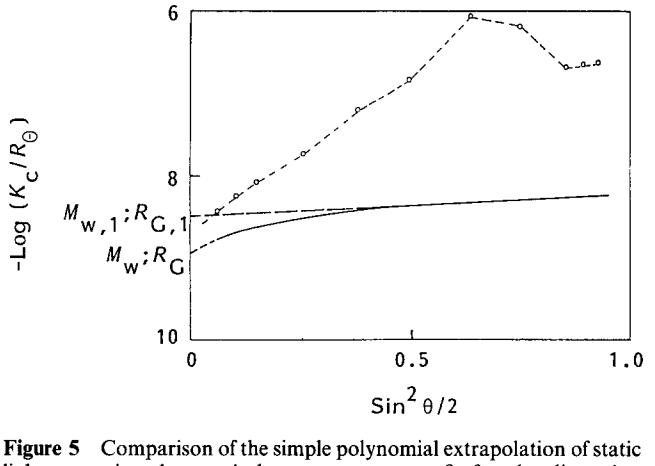

Figure 5 Comparison of the simple polynomial extrapolation of static light scattering data and the two-component fit for the dispersion of sample 1. ——, Angular dependence of K_C/R_Θ (a); results: $M_w = 9.30 \times 10^8$ g mol^{-1}; $R_G = 157$ nm. ——, Fit for component 1 (b); parameters: $M_{w,1} = 3.16 \times 10^8$ g mol^{-1}; $R_{G,1} = 43.2$ nm; ○, (a)–(b) at the fixed angles; – – –, fit for component 2

Table 2 Results of the two-component separation and densities of the body and shell of the particles

Sample	$10^{-8}\ M_{w,1}$ (g mol^{-1})	w_1	$R_{G,1}$ (nm)	$R_{H,1}$ (nm)	d_{body} (g cm^{-3})	d_{cor} (g cm^{-3})	R_{body} (nm)	ρ
X1	1.89	0.9998	34.9	–	1.183	0.149	38.7	–
X2	0.67	0.9994	26.7	–	1.177	0.146	27.4	–
X3	0.51	0.9992	25.5	–	1.171	0.151	24.6	–
X4	0.37	0.9997	20.8	49.3	1.166	0.146	21.8	0.421
1	3.16	0.9647	43.2	–	1.187	0.055	45.5	–
2	2.23	0.9933	38.6	–	1.184	0.098	41.4	–
3	1.07	0.9985	31.8	61.4	1.181	0.099	31.4	0.518
4	0.86	0.9978	26.2	57.3	1.178	0.085	29.8	0.457
5	31.7	0.9636	94.8	134.7	1.188	0.032	108.2	0.704
6	12.5	0.9983	68.2	112.6	1.186	0.069	72.5	0.606
7	6.26	0.9988	51.0	89.4	1.184	0.161	57.8	0.571
8	3.86	0.9989	45.0	80.6	1.182	0.148	49.3	0.558
	10^{-8} $M_{w,1,max}$		$R_{G,1,max}$					
9	75.1	–	121	–	1.188	0.024	137.8	–
10	69.6	–	118	–	1.187	0.022	115.5	–
11	60.9	–	113	–	1.185	0.022	105.0	–
12	41.9	–	100	–	1.184	0.044	103.7	–
13	139	–	148	–	1.189	0.019	171.0	–
14	139	–	148	–	1.188	0.037	200.5	–
15	118	–	140	–	1.186	0.054	186.2	–

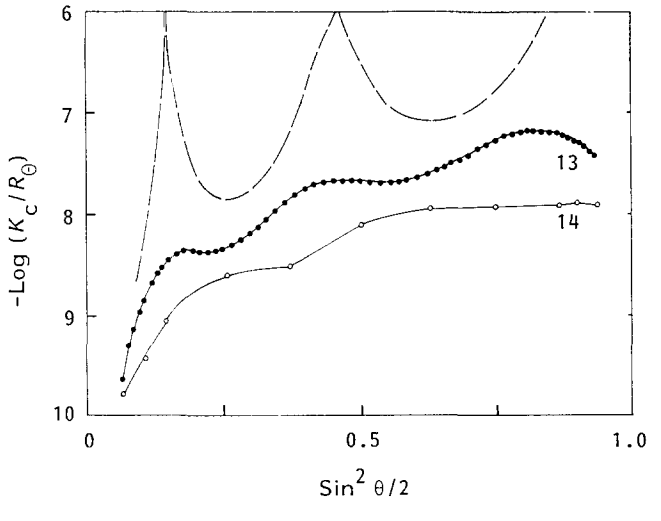

Figure 6 Log(K_C/R) *versus* sin^2(Θ/2): ●, of dispersion 13 ($c = 2.32 \times 10^{-5}$ g cm^{-3}) measured at 61 angles; ——, fit of the position of the maxima by two components; ○, of dispersion 14 ($c = 2.37 \times 10^{-5}$ g cm^{-3}) measured at 11 standard angles

Interpretation of the particle scattering for dispersion particles with R > *140 nm*

For particles with a geometric radius greater than ~140 nm, the calculation can be done with the Rayleigh–Debye–Gans approximation.

We tried to use the two-component separation procedure for dispersion samples 9–11 and 13–15, i.e. those with larger particles. In this case the conditions for an exact fit, especially equation (1), cannot be fulfilled. This result is not connected with the influence of the particle size distribution of the original samples, but exclusively with the unwanted aggregation of particles.

To use the maximum of the scattering intensity is a second possibility for the interpretation. In *Figure 6*, the values log(K_C/R) are plotted for two of the dispersions. According to the non-negligible particle size distribution and to the aggregation in the diluted dispersions, the maxima of the curves are very broad. Therefore an exact determination of the maximum, in order to calculate the average particle size, is impossible.

In these cases we tried to fit the positions of the maxima using Rayleigh's equation for the scattering of spheres (equations (4) and (5)) without calculating the complete scattering behaviour for defined radii of gyration and molar masses. Especially in the difficult case of the interpretation of the two or three maxima, which can be observed for particles with $R_G > 140$ nm, this method leads to sensible results for the dimensions. Nevertheless, a higher resolved measurement allows a reliable interpretation. *Figure 6* also shows log(K_C/R) of dispersion sample 13 measured at 61 angles. In this case we can distinguish between various possible interpretations of the three maxima as belonging to the original sample (the second peak) or caused by aggregation (the first and third peaks).

In order to obtain real values of the particle masses from the radii of gyration, we used the $R_{G,1}/M_w$ relationship and calculated the values $M_{w,max}$ which fit into the picture of sizes, masses and densities instead of the particle mass, which is influenced by aggregation. The data are marked with the index 'max' in *Table 2*.

Separation of components by detailed analysis of the autocorrelation functions

Additionally to the particle scattering function, measured by SLS, the autocorrelation functions of dynamic scattering can be analysed. Time resolution is used as a powerful effect in addition to angular resolution, which acts in both versions of the experiment.

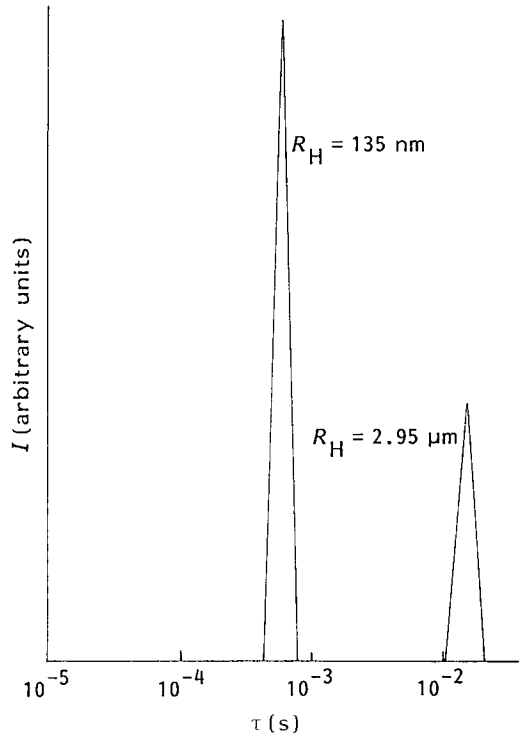

Figure 7 Separation of components of dispersion 5 by the program 'Contin'; $R_{H,1} = 134.7$ nm, $R_{H,2} = 2950$ nm

Using Provencher's program 'Contin'[17] we obtained the $R_{H,1}$ data presented in *Table 2*. An example for this separation is given in *Figure 7*. The squares of $R_{G,1}$, $R_{G,1,max}$ and $R_{H,1}$ are plotted in *Figure 8*. Although the Contin method and the two-component separation method differ strongly in mathematical sense as well as in the physical meaning, the result of these very different calculations is a coherent picture.

The parameter ρ and the corona dimensions and density

The dimensionless parameter[18]:

$$\rho = R_G/R_H \tag{8}$$

clearly reflects the influence of the stabilizer content, especially the dissolved chains of the poly(ethylene-*co*-propylene) part of the stabilizer. The dispersions with low stabilizer content give data close to $\rho = 0.776$, the limit for the hard sphere (*Table 2*).

The parameter ρ is plotted against x_I, the content of poly(ethylene-*co*-propylene) in the dispersion in *Figure 9*. With a decreasing content of stabilizer, ρ grows, whereas at higher contents unexpectedly low ratios are obtained. (Normally for dissolved molecules or parts of such molecules values higher than 0.776 should be obtained.) Such data are published by Kunz *et al.*[19] for microgels of poly(butyl methacrylate). The shell model of the PMMA dispersions is analogous to the concept described above. Nevertheless, in our model the closed curve of the corrected points $\rho = R_{G,1}/R_{H,1}$ (also plotted in *Figure 9*) indicates the possibility of unswollen cores of the dispersion particles, because this curve tends to the value $\rho = 0.776$ for hard spheres. This finding is therefore especially meaningful because both constituent values were determined by independent experiments on different samples and calculated by various mathematical methods of data analysis on different suppositions.

It should always be borne in mind that all the dispersions are not actually monodisperse and all results are obtained by model calculations based on experimental results. They do not agree with the finding of swollen particle bodies[3]. The correctness of one or the other finding can be proved by independent measurements under the experimental conditions of optical masking, i.e. in an isorefractive solvent for the shell chains.

Assuming an unswollen body, the density of the body as an arithmetic average of both components, solid PMMA and polystyrene, can be calculated. Then R_{body} can be evaluated from $M_{w,1}$ and the density of the body:

$$R_{body} = \left(\frac{3(x_P + x_A) M_{w,1}}{4\pi N_A d_{body}} \right)^{1/3} \tag{9}$$

where x_P and x_A are the mass fractions of PMMA and polystyrene, respectively, and N_A is Avogadro's number.

The density of the corona d_{cor} is the difference between

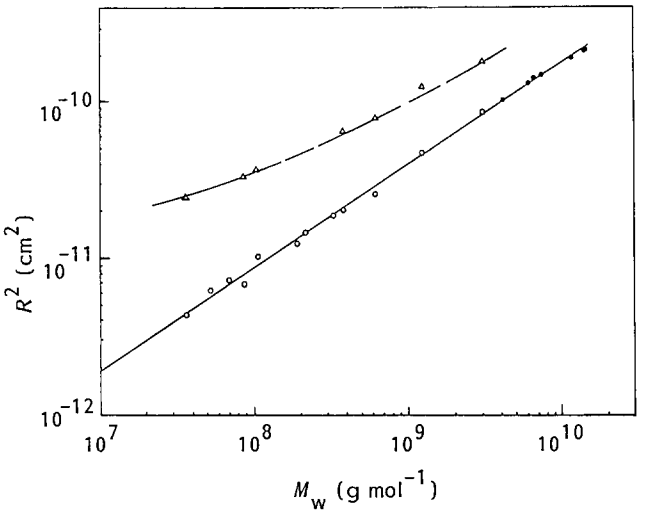

Figure 8 Squares of the radii of gyration $R^2_{G,1}$ (○) and $R_{G,1,max}$ (●), and of hydrodynamic radii $R^2_{H,1}$ (△) *versus* the particle mass $M_{w,1}$ or $M_{w,1,max}$, respectively, for poly(methyl methacrylate) dispersions stabilized by polystyrene-*block*-poly(ethylene-*co*-propylene)

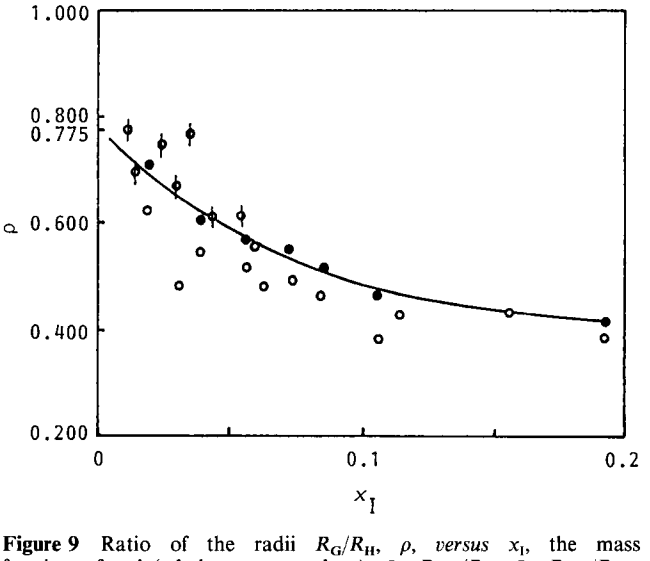

Figure 9 Ratio of the radii R_G/R_H, ρ, *versus* x_I, the mass fraction of poly(ethylene-*co*-propylene): ○, $R_{G,1}/R_H$; ●, $R_{G,1}/R_{H,1}$; ⦶, $R_{G,1,max}/R_H$

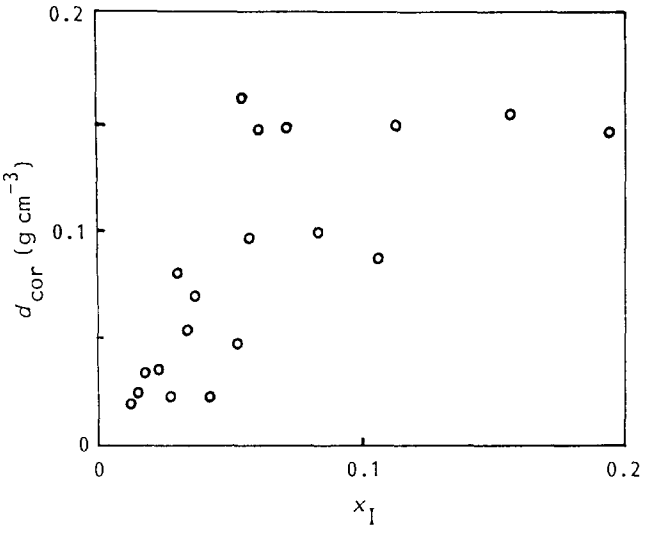

Figure 10 Density of the corona d_{cor} *versus* x_I, the mass fraction of poly(ethylene-*co*-propylene)

the density of the whole particle (obtainable from R_1) and the density of the body:

$$d_{cor} = \frac{3}{4\pi N_A}\left(\frac{x_I M_{w,1}}{R_1^3 - R_{1,body}^3}\right) \quad (10)$$

where x_I is the mass fraction of poly(ethylene-*co*-propylene). The corona densities cover the whole region of sizes and stabilizer contents, i.e. from 0.15 g cm^{-3} for samples with a high stabilizer content, to 0.02–0.04 g cm^{-3} for those with lower contents. In *Figure 10* the densities of the corona, d_{cor}, are plotted against x_I, the mass fractions of the stabilizing poly(ethylene-*co*-propylene). As expected, the density of corona increases with increasing x_I.

CONCLUSIONS

A two-component separation in combination with a fitting procedure on the basis of the Rayleigh particle scattering function of spheres is useful for precise interpretation of the static light scattering data of poly(methyl methacrylate) dispersions. In a similar manner, an analysis of the exponents of autocorrelation functions measured by dynamic light scattering leads to more reliable data for particle sizes. For bigger and more unstable particles the radii of gyration, which were calculated from the positions of the extrema of the intensity of scattering, fit into the picture of sizes and densities over a broad range of molar masses, sizes and densities of particle cores and shells.

ACKNOWLEDGEMENTS

The authors are grateful to Drs Č. Koňák and P. Štěpánek (Prague) for cooperation in dynamic light scattering experiments, and to Dr J. Stejskal, Professor Dr P. Kratochvíl and Dr Z. Tuzar (Prague) for yielding the samples and for helpful discussions. Dr O. Procházka (Prague) permitted the use of the program 'Zimm' for evaluation of static light scattering data, and Dr S. Provencher (Göttingen) the program 'Contin'.

REFERENCES

1 Barett, K. E. J. (Ed.) 'Dispersion Polymerization in Organic Media', Wiley, London, 1975
2 Winnik, M. A., Lukas, R., Chen, W. F., Furlong, P. and Croucher, M. D. *Makromol. Chem., Macromol. Symp.* 1987, **10/11**, 483
3 Stejskal, J., Kratochvíl, P., Koubík, P., Tuzar, Z., Urban, J., Helmstedt, M. and Jenkins, A. D. *Polymer* 1990, **31**, 1816
4 Wallenfels, K., Sund, H. and Burchard, W. *Biochem. Z.* 1962, **335**, 315
5 Kratochvíl, P. *Coll. Czechoslov. Chem. Commun.* 1965, **30**, 1119
6 Lange, H. *Kolloid-Z. Z. Polym.* 1970, **240**, 747
7 Procházka, O., Tuzar, Z. and Kratochvíl, P. *Makromol. Chem.* 1983, **184**, 2097
8 Francuskiewicz, F. and Dautzenberg, H. *Eur. Polym. J.* 1985, **21**, 455
9 Dautzenberg, H. and Rother, G. *J. Polym. Sci. B* 1988, **26**, 353
10 Rayleigh, J. W. *Proc. R. Soc. A* 1914, **90**, 219
11 Stejskal, J., Kratochvíl, P. and Koňák, Č. *Polymer* 1991, **32**, 2435
12 Ochiai, H., Kamata, K. and Murakami, I. *Polym. Commun.* 1984, **25**, 158
13 Helmstedt, M. *Makromol. Chem., Macromol. Symp.* 1988, **18**, 37
14 Morrison, J. D., Grabowski, E. T. and Herb, O. A. *Langmuir* 1985, **1**, 496
15 Shepard, A. F., Henne, A. L. and Midgley, T. Jr *J. Am. Chem. Soc.* 1931, **53**, 1951
16 Dhont, J. K. G. PhD Thesis, Rijksuniversiteit, Utrecht, 1985
17 Provencher, S. W. *Comput. Phys. Commun.* 1982, **27**, 213, 229
18 Burchard, W. *Adv. Polym. Sci.* 1983, **48**, 1
19 Kunz, D., Thurn, A. and Burchard, W. *Colloid Polym. Sci.* 1983, **261**, 635